# Obtaining the Highest Occupied Molecular Orbital Peak of Organic Matter from Photoelectron Yield Spectra

Shohei Tadano,[1] Yasuo Nakayama,[2] Hiroumi Kinjo,[1] Hisao Ishii,[1,3,4] and Peter Krüger[1,3,*]

[1] *Graduate School of Advanced Integration Science, Chiba University, 1-33 Yayoi-cho, Inage-ku, Chiba 263-8522, Japan*

[2] *Department of Pure and Applied Chemistry, Faculty of Science and Technology, Tokyo University of Science, 2641 Yamazaki, Noda 278-8510 Japan*

[3] *Molecular Chirality Research Center, Chiba University, 1-33 Yayoi-cho, Inage-ku, Chiba 263-8522, Japan*

[4] *Center for Frontier Science, Chiba University, 1-33 Yayoi-cho, Inage-ku, Chiba 263-8522, Japan*

(Received 29 January 2019; revised manuscript received 20 March 2019; published 29 May 2019)

We propose a simple theory of photoelectron yield spectra (PYS) on the basis of a density-of-states approximation and universal transmission and loss functions. The theory reproduces the known threshold behavior of metals and that of semiconductors in the indirect-transition regime. We show that a Gaussian-shaped density of states leads to a PYS spectrum that increases very nearly as the third power of energy from threshold, indicating that the empirical cube law of PYS of organic matter reflects the Gaussian-broadened highest occupied molecular orbital peak. We show how the peak position and width can be extracted from the PYS spectrum. The results obtained for several organic compounds agree well with ultraviolet photoemission data. We further show that the density of occupied states is approximately proportional to the second derivative of the PYS spectrum in the near-threshold region.

DOI: 10.1103/PhysRevApplied.11.054081

## I. INTRODUCTION

Photoelectron yield spectroscopy (PYS) is a technique for probing the occupied electronic states and ionization energy of materials [1,2]. Because of its relatively simple experimental setup, it is especially attractive for industrial applications [3]. In a PYS experiment, the total electron yield is measured as a function of the photon energy. Compared to photoelectron spectroscopy (PES), total yield measurements have the advantage of higher sensitivity and larger probing depth. Moreover, there are PYS detection methods that do not require vacuum conditions. This makes PYS especially interesting for materials that are volatile or sensitive to atmospheric conditions, such as organic molecules. However, the relation between the PYS spectrum and the electronic structure of the material is much less direct than in PES. In PYS, the photoemission current is integrated over the photoelectron energy. Consequently, the first derivative of the PYS spectrum is sometimes used for estimating the photoelectron energy distribution and the density of occupied states [3,4]. In practice, PYS is most useful for measuring the work function of metals [5] and the ionization energy of inorganic and organic semiconductors [2] through a simple analysis of the near-threshold spectra. The ionization energy can be found by fitting the near-threshold PYS spectra to a power law:

$$Y(\omega) \propto (\omega - \phi)^n, \quad \omega > \phi, \tag{1}$$

where $Y$ is the measured yield, $\omega$ is the photon energy ($\hbar = 1$), $\phi$ is the threshold energy, and $n$ is the exponent (not necessarily an integer). $\phi$ equals the work function in metals and the ionization energy in molecules. In semiconductors, it is given by the difference between the vacuum level and the valence-band maximum. PYS has been used extensively for measuring the ionization energy of organic films and heterostructures, a crucial quantity for organic electronics [2]. Although the near-threshold PYS spectrum depends on the energy distribution of the low-lying occupied states, this information is generally left unexploited because the proper analysis method is unknown.

The theory of PYS was pioneered by Fowler [5], who correctly described the temperature dependence of PYS in metals by using a free-electron model. At zero temperature, Fowler's theory yields Eq. (1), with $n = 2$. Kane [6] developed a PYS theory for single-crystal semiconductor surfaces based on band theory. He predicted various different threshold behaviors depending on the dominant excitation process, namely direct and indirect band transitions in the bulk or at the surface. As for organic materials, the situation is far less clear. Experimentally, $n \approx 3$ has been found for most organic matter [2,7] An empirical model

*pkruger@chiba-u.jp

 

for the PYS threshold behavior of organic matter was proposed by Kochi *et al.* [7]. They considered emission from the highest occupied molecular orbital (HOMO) level and assumed a linear energy distribution of the emitted electrons due to the Franck-Condon effect. Using a semiempirical transmission function, they deduced a power law with $n = 2.5 - 3$.

In this paper, we derive a simple expression that relates the PYS spectrum to the density of occupied states of the material. This expression reproduces the exact threshold behavior of metals ($n = 2$) and it is consistent with Kane's theory for semiconductors. For a Gaussian-shaped DOS, which describes the HOMO peak of most organic materials well, we show that the PYS spectrum rises very nearly as the cube of the photon energy from threshold. While it is well known that the cube law is the best power-law fit for the near-threshold PYS of organic matter [2], there has been no theoretical explanation for this empirical fact apart from Kochi's model [7]. The present theory provides a different and more general explanation, which recovers the cube law as the limiting behavior at extreme threshold. Based on the PYS spectrum obtained for a Gaussian-shaped DOS, we extract the HOMO-peak position and width from the PYS data of several organic materials and obtain good agreement with photoemission data. Finally, we show that, in general, the DOS is approximately proportional to the second derivative of the PYS spectrum in the near-threshold region.

## II. THEORY

### A. Derivation of a simple PYS expression

To obtain a simple formula for the PYS analysis, we start from the three-step model of photoemission [8]. The photoelectron current $I(E,\omega)$ can be written as follows:

$$I(E,\omega) = P(E,\omega)X(E)T(E).$$

Here, $P$ is the probability that a photon of energy $\omega$ excites an electron to a final state with kinetic energy $E$ (in vacuum). $X$ is the probability that this electron reaches the surface and $T$ is the probability that it is transmitted through the surface. In the independent-particle picture, $P$ is given by Fermi's golden rule:

$$P(E,\omega) = \sum_{if} |V_{if}|^2 \delta(E_f - E_i - \omega)\delta(E - E_f),$$

where $i$ and $f$ run over occupied and unoccupied eigenstates $\psi_i$ and $\psi_f$, respectively, with energies $E_i$ and $E_f$ measured from the vacuum level. $V$ denotes the electron-photon interaction and $V_{if} = \langle \psi_f | V | \psi_i \rangle$ is the optical-transition matrix element. Here, we assume $V_{if}$ to be constant ($= \bar{V}$) for simplicity. This neglect of matrix-element effects is widespread in photoemission and PYS analysis [9]. It is empirically justified by the fact that the spectral shape resembles a suitably broadened occupied DOS [10]. Moreover, we are mainly interested in the low-lying states of organic matter, which are essentially of a carbon $p$ character. In this case, the energy dependence of $V_{if}$ is weak because there is only a single atomic cross section involved [11]. We then obtain the following:

$$P(E,\omega) \approx |\bar{V}|^2 D(E-\omega)D(E), \quad E > 0, \omega > -E_F,$$

where $D(E-\omega)$ is the initial and $D(E)$ the final density of states (DOS). The propagation term $X(E)$ accounts for losses due to inelastic collisions. In ultraviolet photoemission, $X(E)$ is approximately proportional to the electron mean free path $\lambda(E)$ [10], and we obtain

$$I(E,\omega) \propto D(E-\omega)D(E)\lambda(E)T(E). \tag{2}$$

The total photoelectron yield $Y(\omega)$ is the number of photoemitted electrons per absorbed photon. The photoabsorption coefficient varies slowly with the photon energy around the photoemission threshold ($\omega \approx \phi$) [6,7]. Therefore, the photoelectron yield in the near-threshold region is essentially proportional to the integrated PES spectrum:

$$Y(\omega) \propto \int_0^{\omega-\phi} I(E,\omega)dE. \tag{3}$$

At a glance, Eq. (3) suggests that the PES spectrum can approximately be obtained from the first derivative of the PYS spectrum. This much used procedure [3] is reasonable sufficiently far from threshold ($\omega \gg \phi$), where the photocurrent $I(E,\omega)$ varies slowly with the photon energy $\omega$. However, here we focus on the spectral region up to 1–2 eV above threshold, which probes the states close to the Fermi level. In this case, $I(E,\omega)$ varies quickly with $\omega$ and the PYS spectrum is better described by the second derivative of $Y(\omega)$ than by the first one, as we show below. In the following, we assume that the density of final states varies slowly with energy above the vacuum level and $D(E)$ can thus be replaced by a constant in the PYS threshold region. This is reasonable, because final-state resonances are usually located below the vacuum level. We then obtain the following:

$$Y(\omega) \propto \int_0^{\omega-\phi} D(E-\omega)\lambda(E)T(E)dE. \tag{4}$$

The inelastic mean free path $\lambda(E)$ is well described by the universal function $\lambda(E) = A/(E+\phi)^2 + B\sqrt{E+\phi}$ [12], where $\phi = -E_F$. This function will be used in the quantitative analysis for organic matter below. However, to obtain a simple formula for the near-threshold region, we approximate $\lambda(E)$ by a constant in the following. The transmission function $T(E)$ is zero below threshold

($E < 0$), increases, and approaches 1 for high energy, when all electrons reaching the surface are emitted. In the low-energy limit relevant for PYS, we can assume that $T(E)$ increases linearly with $E$ above threshold. This follows from the semiclassical escape-cone argument [10], which remains valid quantum mechanically when assuming free-electron dispersion for the final states inside matter, $E(\mathbf{k}) = -V_0 + \hbar^2 k^2/2m$, where $V_0$ is the inner potential, corresponding to the surface potential barrier. From energy and parallel momentum conservation, we have $k_z' = \pm\sqrt{k_z^2 - 2mV_0/\hbar^2}$, where $k_z$ ($k_z'$) is the surface-normal photoelectron momentum in matter (in vacuum). The electron escapes if $k_z' > 0$ or, equivalently, if $\cos\theta \equiv k_z/k > 1/\sqrt{1+E/V_0} \equiv \cos\theta_c$, i.e., if the polar angle $\theta$ of the momentum vector inside matter is smaller than the critical value $\theta_c$. The transmission probability is then given by the following:

$$T(E) = \int_+ g(E,\Omega)\Theta(\theta_c - \theta)d\Omega \Big/ \int_+ g(E,\Omega)d\Omega\ ,$$

where $g(E,\Omega)$ is the number of final states inside matter with energy $E$ and momentum direction $\Omega$ (solid angle), and the integration $\int_+$ is over the upper hemisphere ($\theta < \pi/2$) corresponding to electrons with positive normal velocity. $\Theta(x)$ is the Heaviside step function. Defining $f(u) \equiv \int g(E,\Omega)d\phi$, $u \equiv \cos\theta$, we can simplify to $T(E) = \int_{u_c}^1 f(u)du / \int_0^1 f(u)du$, where $u_c = \cos\theta_c$. We now assume that $f(u)$ is constant and obtain the following:

$$T(E) = 1 - \frac{1}{\sqrt{1+E/V_0}} = \frac{E}{2V_0} + O[(E/V_0)^2]. \quad (5)$$

Constant $f(u)$ corresponds to a uniform final-state momentum distribution. This holds trivially for amorphous and polycrystalline matter and also approximately at single-crystal surfaces when the momentum information is blurred by scattering at phonons or lattice imperfections.

As seen from Eq. (5), $T(E)$ is approximately linear near threshold; more precisely, for $E \ll V_0$. The inner potential $V_0$ can be identified with the difference between the vacuum level and the interstitial potential, i.e., the average crystal potential between atomic spheres, which is typically $V_0 = 10 - 20$ eV [10]. For $V_0 = 15$ eV and an energy of 2 eV above threshold, the error of the linear approximation in Eq. (5) is 10%. Focusing on the threshold behavior, we now keep only the leading terms of $T(E)$ (linear) and $\lambda(E)$ (constant). Equation (4) then becomes the following:

$$Y(\omega) \propto \int_0^{\omega-\phi} D(E-\omega)EdE. \quad (6)$$

We first consider the case in which the DOS varies as a power law with binding energy $\omega - \phi - E$, that is, $D(E-\omega) \propto (\omega - \phi - E)^m$ with some exponent $m \geq 0$. By evaluating the integral (6), we then obtain the following:

$$Y(\omega) \propto (\omega - \phi)^{m+2}, \quad (7)$$

i.e., the empirical power law (1) with $n = m + 2$, in agreement with Apker *et al.* [13]. Metals have a finite DOS at $E_F$. To lowest order, the DOS below $E_F$ is constant, so $m = 0$ and we recover the $n = 2$ power law of Fowler [5], obtained with the free-electron model. Semiconductors have a filled parabolic valence band, which leads to a DOS with $m = 1/2$ and thus $n = 5/2$. This exponent agrees with Kane's result for indirect transitions in the bulk [6], which should dominate the threshold behavior in most cases. Indeed, while Kane found exponents varying from $n = 1$ to $n = 5/2$ depending on the transition process, the $n = 5/2$ result is the most general one, valid for "any form of indirect scattering mechanisms" [6]. In our language, indirect scattering (at phonons, crystal imperfections or surface roughness) leads to a constant angular distribution of $g(E,\Omega)$, which is a sufficient condition for Eq. (5). We conclude that our simple theory can explain the known PYS threshold behavior of metals and most semiconductors.

### B. Extracting the DOS from the PYS spectrum

In order to obtain the DOS $D(E)$ from the measured PYS spectrum $Y(\omega)$, we need to "invert" Eq. (4). This can be done by solving the integral equation numerically. Alternatively, a good approximate solution can be obtained from the second derivative of the PYS spectrum, as we now show. Defining $S \equiv \lambda T$, we rewrite Eq. (4) as $Y(\omega) \propto \int_\phi^\omega D(-x)S(\omega - x)dx$, $x = \omega - E$, and obtain the following:

$$Y''(\omega) \propto -D'(-\omega)S(0) + D(-\omega)S'(0) + \int_\phi^\omega D(-x)S''(\omega - x)dx, \quad (8)$$

where $f'$ and $f''$ denote the first and second derivatives of a function $f$, respectively. Since $\lambda(E) > 0$ and $T(E)$ rises from $T(0) = 0$, we have $S(0) = 0$, $S'(0) > 0$ and Eq. (8) can be solved for $D$ as follows:

$$D(-\omega) = Y''(\omega) - R(\omega),$$
$$R(\omega) \equiv \frac{1}{S'(0)} \int_\phi^\omega D(-x)S''(\omega - x)dx, \quad (9)$$

where the unknown proportionality constant of Eq. (8) has been arbitrarily set to $1/S'(0)$, i.e., $D$ in Eq. (9) is not normalized. Equation (9) can be solved iteratively for $D(\omega)$ with initial condition $R(\omega) = 0$. This provides an alternative to solving the integral equation (4).

Importantly, the term $R(\omega)$ is negligible near threshold ($\omega \approx \phi$), because the integration domain is small and $S''/S'(0) \ll 1$, since $S$ is nearly linear. Thus, the occupied DOS is approximately proportional to the second derivative of the PYS spectrum:

$$D(-\omega) \approx Y''(\omega). \tag{10}$$

In the application below, we find that $R$ is indeed very small up to 2 eV above threshold. For higher energies, $S$ flattens off ($S'' < 0$) and so $R$ is a slowly increasing positive contribution. Also, when $S = \lambda T$ is constant, it is directly evident from Eq. (4) that the DOS is proportional to the first derivative of $Y$. As already mentioned above, this is a reasonable approximation sufficiently far from threshold, where $S$ varies slowly. It must be stressed, however, that the first derivative, although useful in practice [3,4] does not lead to the correct threshold behavior. This is obvious when looking at the case of a metal, which is characterized by a finite DOS at $E_F = -\phi$, i.e., $D(-\phi) > 0$. The leading term of the PYS spectrum goes like $Y(\omega) \propto (\omega - \phi)^2$ [5] near threshold, implying $Y'(\phi) = 0$ and $Y''(\phi) > 0$. So it is the second derivative of the PYS signal that has the same threshold behavior as the DOS, rather than the first derivative.

### C. PYS spectrum for a Gaussian-shaped DOS

Our main purpose is the analysis of PYS data of organic matter, where the DOS is often well described as a sum of Gaussian-shaped peaks corresponding to the broadened molecular levels. The broadening may have various causes, including band formation, Frank-Condon-type coupling to molecular vibrations, spatial variations of the electronic potential due to defects and disorder, and the population of phonons at finite temperature. While the precise peak shape depends on the details of the broadening mechanism, the Gaussian shape is appropriate for finite experimental resolution and structural disorder and is a good approximation for vibrational broadening. In the case of intermolecular bond formation or different chemical environments, the HOMO level will be split [14] and the resulting total HOMO-derived DOS feature will not be Gaussian distributed. In this case, the HOMO-peak extraction method described below will usually yield the first peak of the HOMO feature.

First, we show that a Gaussian-shaped DOS leads to a PYS spectrum the threshold behavior of which is very close to a cube law, i.e., to Eq. (1) with $n \approx 3$. We consider a DOS made of a single Gaussian peak centered at $\epsilon_0$ and with standard deviation $\sigma$, i.e., $D(E) = \exp[-(E - \epsilon_0)^2/2\sigma^2]$. In the linear approximation [Eq. (6)], the corresponding PYS spectrum can be obtained in closed form. We assume that the Gaussian (HOMO) peak is fully occupied, i.e., $(E_F - \epsilon_0)/\sigma \gg 1$. In this case, we can extend the upper integration bound in Eq. (6) to infinity and obtain the following:

$$Y(\omega) \propto \sigma^2 \exp\left(-\frac{(\omega+\epsilon_0)^2}{2\sigma^2}\right) + \sqrt{\frac{\pi}{2}}\sigma(\omega+\epsilon_0)\,\mathrm{erfc}\left(-\frac{\omega+\epsilon_0}{\sqrt{2}\sigma}\right), \tag{11}$$

where $\mathrm{erfc}(x) \equiv 1 - \mathrm{erf}(x)$ is the complementary error function. The computed PYS yield is shown in Fig. 1(red line) for $\epsilon_0 = -5.0$ and $\sigma = 0.2$. We have fitted this spectrum with the general threshold power law [Eq. (1)] in the energy range $(-\epsilon_0 - 5\sigma, -\epsilon_0 + \sigma)$, which covers the whole low-energy tail and over 80% of the Gaussian intensity. The fit is excellent, as seen in Fig. 1(a) (blue line). A small disagreement exists around threshold ($\phi$), which appears strongly amplified in the $Y^{1/3}$ plot [Fig. 1(b)]. However, such small differences are usually below noise level, as will be seen in the next section. The best-fit parameters are $n = 2.95 \pm 0.04$ and $\phi = -\epsilon_0 - a\sigma$, with $a = 2.45 \pm 0.04$. The values $n$ and $a$ depend somewhat on the energy range used in the fit, but they are independent of $\epsilon_0$ and $\sigma$, i.e., they are the same for all Gaussian peaks. This result clearly shows that a Gaussian-shaped DOS leads to a PYS spectrum the threshold behavior of which is very close to a cube law ($n = 3$), observed in most organic matter [2,7]. Moreover, we find that the threshold $\phi$, obtained from the standard cube-law fit, is related to the Gaussian parameters by $\phi = -\epsilon_0 - 2.45\sigma$ [see Fig. 1(b)].

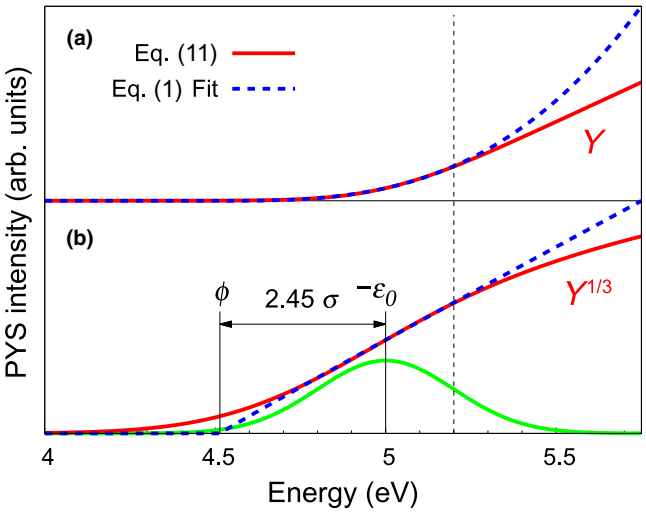


FIG. 1. The PYS spectrum (red solid lines) calculated using Eq. (11) and fitted to the general power law given in Eq. (1) (blue broken lines), with $-\epsilon_0 = 5.0$ and $\sigma = 0.2$. (a) Linear intensity scale ($Y$). (b) Cube-root intensity scale ($Y^{1/3}$). The best-fit parameters are $n = 2.95$ and $\phi = 4.51 = -\epsilon_0 - 2.45\sigma$. The vertical dotted line marks the upper bound of the fitting region. The underlying Gaussian DOS is also shown (green solid line).

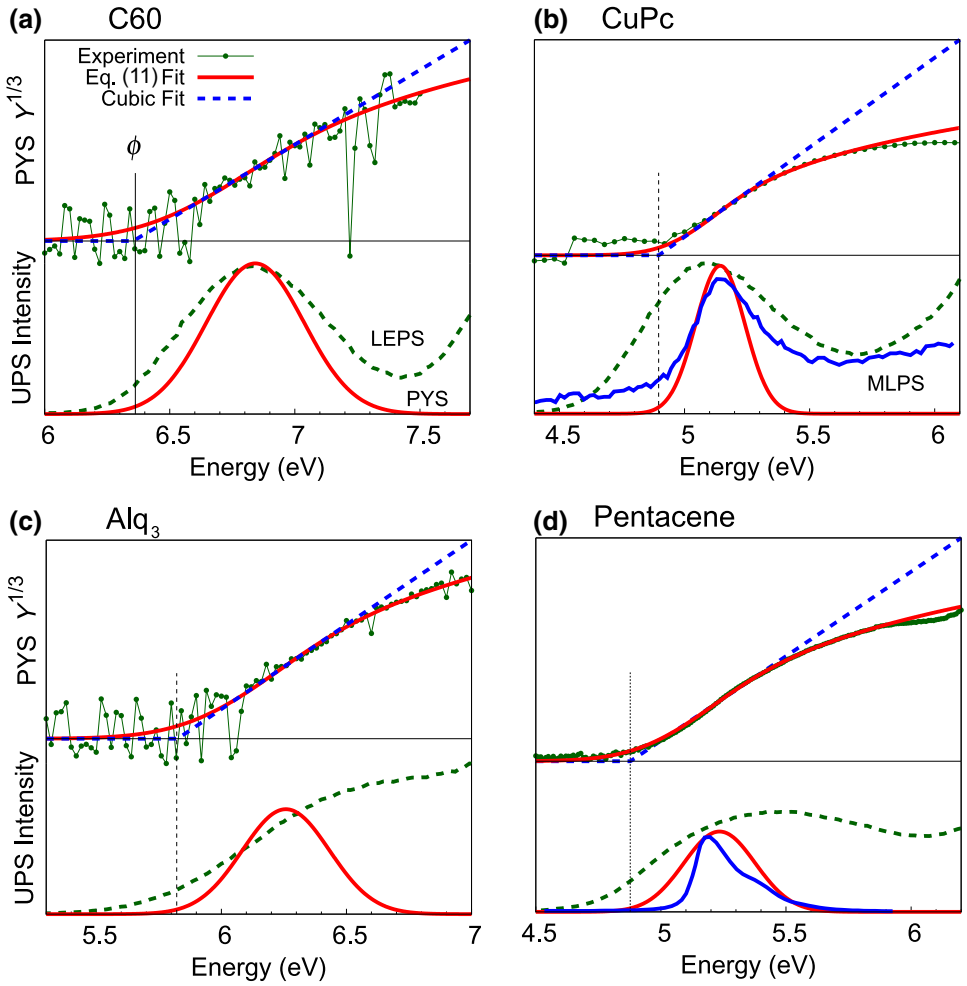


FIG. 2. The PYS analysis of several organic solids. The top panels show the experimental PYS data (green symbols), the fit to Eq. (11) (red solid lines), and the fit to the cube law (blue dotted lines) on a $Y^{1/3}$ scale. In the lower panels, the HOMO peaks extracted from the PYS data (PYS, red solid lines) are compared with low-energy UPS spectra of the same samples (LEPS, green dotted lines) and with high-resolution spectra of monolayer samples [15,16] (MLPS, blue solid lines). The MLPS spectra have been aligned with the PYS peak.

According to Eq. (7), an exact cube law corresponds to a DOS that rises linearly from threshold ($m = 1$). Such a linear photoelectron intensity distribution was effectively assumed by Kochi *et al.* [7] for organic matter. In the light of the present findings, a linear DOS appears as a rough approximation of the rising slope of a typically Gaussian-shaped HOMO peak. In Fig. 1, the PYS spectrum of Eq. (11) (red line) starts to significantly differ from the cube law (blue line) at about 0.8 eV above threshold $\phi$. Qualitatively the same deviation from the cube law is observed in all experimental PYS spectra in Fig. 2 below.

## III. APPLICATION TO ORGANIC SOLIDS

### A. Determination of HOMO peak from PYS data

We apply the above theory to several organic solids, namely fullerene (C60), copper phthalocyanine (CuPc), tris(8-hydroxyquinolinato)aluminum ($Alq_3$), and pentacene. The samples are deposited under ultrahigh vacuum conditions on an indium tin oxide substrate of work function 4.5 eV. The film thicknesses are 60 nm (C60), 30 nm (CuPc), 30 nm ($Alq_3$), and 100 nm (pentacene). The light is unpolarized and impinging in normal incidence. For further experimental details, see Refs. [17] and [18]. The PYS analysis for these systems is shown in Fig. 2. In the upper part of each panel, the experimental PYS data are fitted to Eq. (11) which in turn is fitted to the cube law. The $y$ scale is the cube root of the PYS intensity ($Y^{1/3}$). We see that Eq. (11) agrees very well with the data over the whole energy range, i.e., up to about 1.2 eV above threshold. The difference between the experimental and the theoretical curves is entirely due to noise in the data, which is obvious when looking at pentacene, where the noise is lowest and the agreement is virtually perfect. Thus, Fig. 2

is clear experimental evidence that the near-threshold PYS spectra of organic matter are well described by Eq. (11), reflecting a Gaussianlike-shaped DOS and a linear transmission function [Eq. (6)]. When looking at the cube-law fit (blue lines), we see that it agrees well in the threshold region but starts to deviate strongly from the data around 0.6 eV above threshold. This shows that the cube law is suitable for determining the PYS threshold [2] but that it fails to describe the spectral shape beyond some 0.5 eV.

The Gaussian peak, obtained from the fit to Eq. (11), is plotted in the lower panels (red lines) and denoted "PYS peak" in the following. We note that the fitting results (peak position and width) depend slightly on the energy range used in the fit. As a rule of thumb, the upper limit should not exceed the peak position by more than $3\sigma$, which is about 0.5 eV for the present systems. If a wider energy range is used, overlap with higher-energy peaks may worsen the fit. In Fig. 2, the PYS peaks are compared with ultraviolet photoemission spectra. The green solid lines (labeled LEPS) have been recorded *in situ* with a low photon energy of 7.7 eV (except for C60, 8.0 eV) and are plotted as a function of the binding energy measured from the vacuum level. The curves labeled MLPS are high-resolution ultraviolet photoemission spectra (UPS) of monolayer samples. They have been shifted in energy with respect to the LEPS spectra in order to compensate for the different ionization potential, due to different layer thicknesses and substrates.

The peak positions of the LEPS spectra agree well with the PYS peaks. This shows that the peak extracted from the PYS spectrum indeed corresponds to the HOMO peak of these organic solids. The LEPS peak widths are, however, larger by a factor of 1.5–2.5 than the PYS values. The peak widths are summarized in Table I.

The large peak widths of the LEPS data are partly due to the limited energy resolution with an instrumental broadening of about 0.23 eV [19]. This is supported by the fact that the UPS spectra of the $Alq_3$ and pentacene films recorded with high-resolution equipment and approximately 20 eV photon energy [20,21], have HOMO peaks that are smaller by 0.2–0.3 eV (see the HEPS data in Table I). Nonetheless, all peak widths from UPS data of film samples (LEPS, HEPS), are considerably larger than the PYS widths. Interestingly, however, the HOMO-peak widths of the CuPc and pentacene monolayer spectra (MLPS) are very close to the corresponding PYS values. This suggests that the peak widths obtained by the present PYS analysis correspond to the intrinsic width of the molecular HOMO level, while the UPS peaks of film samples are further broadened by solid-state effects related to intermolecular interaction and disorder. The systematically larger UPS peak width of films as compared to monolayers has previously been attributed to the difference in electronic polarization between the outermost surface layer and the "bulk" of the film [16,22]. Due to the extreme surface sensitivity of UPS, the peak shift of the surface layer of up to 0.3 eV [22] leads to substantial broadening of the spectrum. Also, structural disorder and the so-called "charge-up" effect upon photoionization give rise to a nonuniform electrostatic potential and lead to further broadening. These broadening effects can be expected to be weaker in PYS than in UPS for the following reasons. First, UPS is extremely surface sensitive, with a probing width of about 1 nm, corresponding to only two or three molecular layers. In PYS, the collected electrons have a very low kinetic energy and thus a relatively large escape depth of about 5 nm [12]. The PYS spectrum therefore probes mainly the inner layers of the film and it is less affected by the polarization-induced peak shift of the surface layer [22]. Second, PYS is less sensitive than UPS to surface roughness and the resulting variation of the electrostatic potential within the surface plane. In UPS, spatial variations of the binding energy of the molecular level lead to peak broadening, since UPS is measured with respect to the fixed Fermi level of the electron detector. PYS, in contrast, is sensitive only to the local ionization energy, relative to the *local* vacuum level. Since a change in electrostatic potential shifts both the molecular level and the local vacuum level, the variation of the local ionization energy is small and so the broadening of the PYS peak is smaller than in UPS. These arguments indicate that the PYS peaks are less affected by surface-related broadening effects than UPS, which partly explains their systematically smaller width. Often, the HOMO feature is made of overlapping peaks, shifted by polarization or band and/or bond formation [14]. The good agreement of the PYS peak widths with the MLPS data suggests that, for such a composite HOMO band, the PYS peak corresponds to a single component, namely the one with the lowest binding energy. Clear evidence for this interpretation is provided in the case of pentacene in the next section.

Let us note that the Gaussian shape of the HOMO peak is an approximation that cannot account for fine structures such as the single-molecule vibrational peaks seen, e.g., in the MLPS spectrum of pentacene (Fig. 2, [16]) or the HOMO band dispersions observed in photoemission

TABLE I. The HOMO-peak widths [full width at half maximum (FWHM), in eV] of the investigated organic compounds. The PYS and low-energy photoemission (LEPS) are from this work. The high-energy photoemission data of films (HEPS) and monolayers (MLPS) were taken from (b) Ref. [15], (c) Ref. [20], (d) Ref. [21], and (d') Ref. [16].

| | (a) C60 | (b) CuPc | (c) $Alq_3$ | (d) Pentacene |
|---|---|---|---|---|
| PYS | 0.47 | 0.24 | 0.52 | 0.28 |
| LEPS | 0.71 | 0.59 | 1.2 | 0.82 |
| HEPS | | | 1.05[c] | 0.57[d] |
| MLPS | | 0.31[b] | | 0.23[d'] |

of single-crystal films [23]. Therefore, the present analysis method should only be applied to noncrystalline or polycrystalline samples.

### B. DOS estimation by second derivative or deconvolution of PYS signal

Here, we use the second derivative of the PYS spectrum [Eq. (10)] to estimate the near-threshold DOS without assumptions on its shape. As the noise-over-signal ratio becomes hugely amplified upon numerical differentiation, the second-derivative method can only be applied to high-resolution low-noise data. Among the four systems in Fig. 2, only the pentacene data can be used. The raw PYS spectrum of pentacene (green line Fig. 2) is smoothened using a spline function and the control parameter (the root-mean-square error) is chosen to be as small as possible. The result is shown in Fig. 3. For comparison, the DOS is also extracted from the PYS data by numerically solving the integral equation (4) (curve labeled "Deconvolution"). Here, we use the full $T(E)$ function in Eq. (5) and the universal function for the inelastic mean free path $\lambda(E) = A/(E - E_F)^2 + B\sqrt{E - E_F}$ with $A = 31$ and $B = 0.087$ appropriate for organic matter [12]. For the other two parameters, we take typical values $V_0 = 10$ eV and $E_F = -5$ eV. The Gaussian fit ["Eq. (11) Fit," the same as in Fig. 2] and a high-energy photoemission spectrum ("HEPS") of a different polycrystalline pentacene film sample [21] are also shown in Fig. 3. We first note that the DOS obtained by second derivative of the PYS signal agrees very well with the numerical deconvolution except that the intensity of the second derivative is somewhat reduced at higher energy, because the positive term $R(\omega)$ in Eq. (9) is neglected. The close agreement between

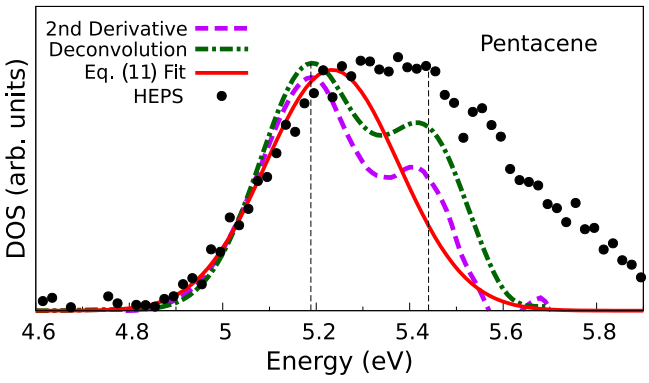


FIG. 3. DOS extraction from PYS of pentacene. The raw PYS data is shown in Fig. 2. The DOS obtained by second derivative (purple) and numerical deconvolution (green) of the PYS data is compared with the Gaussian peak ["Eq. (11) fit," red, the same as in Fig. 2(d)] and the high-resolution photoemission spectrum of a pentacene film obtained with synchrotron light ("HEPS") [21]. The thin dotted lines mark the peak positions obtained by a Gaussian decomposition of the "Deconvolution" curve.

the second derivative and the deconvolution method is also found for PYS data from single-crystal rubrene (not shown) on an energy range up to 2 eV from threshold. As mentioned above, the second-derivative analysis can be numerically delicate because of noise amplification. If the raw data is too noisy, the deconvolution method should be used instead. Note that the extraction of the HOMO-peak position and width introduced in the previous section is free of such numerical problems. It does not involve any derivatives, but only a least-squares fit of the simple analytic expression (11) to the data, which is a very stable numerical operation.

The "2nd Derivative" and "Deconvolution" DOS in Fig. 3 show two overlapping peaks, split by 0.25 eV. This peak splitting compares well with the experimentally and theoretically established fact that the HOMO of pentacene is made of two narrow bands, split by $0.1 \sim 0.4$ eV depending on the momentum vector and the crystal phase [24–26]. The extracted DOS agrees also well with the photoemission data ("HEPS") in terms of the position and width of the central part. It is seen from Fig. 3, that the single Gaussian peak ("Eq. 11 Fit") corresponds to the first of the two overlapping peaks of the HOMO feature. Also note that the single Gaussian peak fits remarkably well with the low-energy part ($E < 5.25$ eV) of the HEPS HOMO signal. From this analysis, we conclude that in case of a broad HOMO band made of several overlapping peaks, the PYS peak obtained by fitting to Eq. (11) corresponds to the lowest energy peak. Higher-energy features of the DOS can approximately be extracted from high-resolution PYS data by second derivative or numerical deconvolution.

## IV. CONCLUSIONS

In summary, we propose a method for estimating the DOS of the highest occupied states of organic matter from PYS data. This provides important electronic information beyond the standard determination of the ionization potential. The PYS spectrum is approximated by an energy integral over the occupied density of states of the system, weighted by a transmission and loss function, which scales linearly near threshold. This simple general theory reproduces the known threshold behaviors of metals and most semiconductors. We show that a Gaussian-shaped DOS leads to a PYS spectrum that is very close to a cube law near threshold. As the HOMO peak of organic matter is very often of approximately Gaussian shape, we thus explain the empirical fact that a cube law fits the PYS threshold behavior of most organic materials well. We propose a simple method for extracting the HOMO-peak position and width from the PYS spectrum. By analyzing the PYS data of several organic films, we obtain HOMO peaks that are in good agreement with the available UPS data. For film samples, the PYS-derived peak widths are narrower than the corresponding UPS peaks and agree well

with monolayer UPS data. This indicates that PYS-derived peaks are less sensitive than UPS peaks to broadening induced by intermolecular polarization and disorder. In the case of overlapping peaks, the PYS-derived peak corresponds to the lowest binding-energy component of the HOMO band. DOS features beyond the first peak can be estimated through the second derivative or numerical deconvolution of the PYS signal.

## ACKNOWLEDGMENTS

This work was supported by JSPS KAKENHI Grants No. JP15H05498 and No. JP16K05393.

[1] M. Pope, and C. E. Swenberg, *Electronic Processes in Organic Crystrals and Polymers* (Oxford Science, Berlin, 1999), 2nd ed., Chap. 4

[2] H. Ishii, H. Kinjo, T. Sato, S. Machida, and Y. Nakayama, *Electronic Processes in Organic Electronics: Bridging Nanostructure, Electronic States and Device Properties* (Springer, Berlin, 2015), Chap. 8, p. 131

[3] Catalog of Surface Analyzer AC-2 by Riken Keiki Co., Ltd. http://www.rikenkeiki.co.jp/english/products/detail/15.

[4] A. Ohta, N. X. Truyen, N. Fujimura, M. Ikeda, K. Makihara, and S. Miyazaki, Total photoelectron yield spectroscopy of energy distribution of electronic states density at GaN surface and $SiO_2$/GaN interface, Jpn. J. Appl. Phys. **57**, 06KA08 (2018).

[5] R. H. Fowler, The analysis of photoelectric sensitivity curves for clean metals at various temperatures, Phys. Rev. **38**, 45 (1931).

[6] E. O. Kane, Theory of photoelectric emission from semiconductors, Phys. Rev. **127**, 131 (1962).

[7] M. Kochi, Y. Harada, T. Hirooka, and H. Inokuchi, Photoemission from organic crystal in vacuum ultraviolet region IV, Bull. Chem. Soc. Jpn. **43**, 2690 (1970).

[8] C. N. Berglund and W. E. Spicer, Photoemission studies of copper and silver: Theory, Phys. Rev. **136**, A1030 (1964).

[9] K. Winer, I. Hirabayashi, and L. Ley, Exponential Conduction-Band Tail in P-Doped a-Si:H, Phys. Rev. Lett. **60**, 2697 (1988).

[10] S. Hüfner, *Photoelectron Spectroscopy: Principles and Applications*, 3rd ed. (Springer, Berlin, 2003).

[11] S. Goldberg, C. Fadley, and S. Kono, Photoionization cross-sections for atomic orbitals with random and fixed spatial orientation, J. Electron Spectros. Relat. Phenomena **21**, 285 (1981).

[12] M. P. Seah and W. A. Dench, Quantitative electron spectroscopy of surfaces: A standard data base for electron inelastic mean free paths in solids, Surf. Interface Anal. **1**, 2 (1979).

[13] L. Apker, E. Taft, and J. Dickey, Photoelectric emission and contact potentials of semiconductors, Phys. Rev. **74**, 1462 (1948).

[14] S. Kera, H. Fukagawa, T. Kataoka, S. Hosoumi, H. Yamane, and N. Ueno, Spectroscopic evidence of strong π-π interorbital interaction in a lead-phthalocyanine bilayer film attributed to the dimer nanostructure, Phys. Rev. B **75**, 121305(R) (2007).

[15] S. Kera, Y. Yabuuchi, H. Yamane, H. Setoyama, K. K. Okudaira, A. Kahn, and N. Ueno, Impact of an interface dipole layer on molecular level alignment at an organic-conductor interface studied by ultraviolet photoemission spectroscopy, Phys. Rev. B **70**, 085304 (2004).

[16] H. Yamane, S. Nagamatsu, H. Fukagawa, S. Kera, R. Friedlein, K. K. Okudaira, and N. Ueno, Hole-vibration coupling of the highest occupied state in pentacene thin films, Phys. Rev. B **72**, 153412 (2005).

[17] H. Kinjo, T. S. H. Lim, Y. Noguchi, Y. Nakayama, and H. Ishii, Significant relaxation of residual negative carrier in polar $Alq_3$ film directly detected by high-sensitivity photoemission, Appl. Phys. Express **9**, 021601 (2016).

[18] T. Sato, H. Kinjo, J. Yamazaki, and H. Ishii, $10^{15}$ $cm^{-3}$ $eV^{-1}$ level detection of density of states of a p-type polymer by $h\nu$-dependent high-sensitivity ultraviolet photoemission spectroscopy, Appl. Phys. Express **10**, 011602 (2016).

[19] Y. Nakayama, T. L. Nguyen, Y. Ozawa, S. Machida, T. Sato, H. Tokairin, Y. Noguchi, and H. Ishii, Complete demonstration of the valence electronic structure inside a practical organic solar cell probed by low energy photoemission, Adv. Energy Mater. **4**, 1301354 (2014).

[20] Y. Nakayama, F. Minagawa, and M. Hikasa, Effects of Water Exposure on Materials for Organic Light Emitting Diodes, UVSOR Activity Report (2018).

[21] Y. Nakayama, Y. Uragami, M. Yamamoto, S. Machida, H. Kinjo, K. Mase, K. R. Koswattage, and H. Ishii, Determination of the highest occupied molecular orbital energy of pentacene single crystals by ultraviolet photoelectron and photoelectron yield spectroscopies, Jpn. J. Appl. Phys. **53**, 01AD03 (2014).

[22] W. R. Salaneck, Intermolecular Relaxation Energies in Anthracene, Phys. Rev. Lett. **40**, 60 (1978).

[23] S. I. Machida, Y. Nakayama, S. Duhm, X. Qian, A. Funakoshi, N. Ogawara, S. Kera, N. Ueno, and H. Ishii, Highest-Occupied-Molecular-Orbital Band Dispersion of Rubrene Single Crystals as Observed by Angle-Resolved Ultraviolet Photoelectron Spectroscopy, Phys. Rev. Lett. **104**, 156401 (2010).

[24] K. Hummer and C. Ambrosch-Draxl, Electronic properties of oligoacenes from first principles, Phys. Rev. B **72**, 205205 (2005).

[25] H. Kakuta, T. Hirahara, I. Matsuda, T. Nagao, S. Hasegawa, N. Ueno, and K. Sakamoto, Electronic Structures of the Highest Occupied Molecular Orbital Bands of a Pentacene Ultrathin Film, Phys. Rev. Lett. **98**, 247601 (2007).

[26] Y. Nakayama, Y. Mizuno, M. Hikasa, M. Yamamoto, M. Matsunami, S. Ideta, K. Tanaka, H. Ishii, and N. Ueno, Single-crystal pentacene valence-band dispersion and its temperature dependence, J. Phys. Chem. Lett. **8**, 1259 (2017).